

· 实验研究 Experimental research ·

兔 VX2 肝转移瘤影像学表现与病理结构
对照研究

史 博, 李智岗, 李亚洲, 王永中, 平 勇, 吴勇超, 郝晓光

【摘要】 目的 探讨兔肝转移瘤模型血供来源及其影像学表现与病理结构的关系。**方法** 新西兰大白兔 40 只,于脾脏种植 VX2 肿瘤细胞悬液 1 ml,浓度 $1 \times 10^7/\text{ml}$ 。瘤株接种后第 14 天作 CT 灌注扫描,第 15 天作 DSA 造影,分别观察肝转移瘤数目及大小,测定 CT 灌注成像转移瘤中心区域、转移瘤边缘及瘤周正常肝组织血流量(BF)、血容量(BV)、肝动脉供血分数(HAF),计算肝动脉灌注量(HAP)和门静脉灌注量(PVP);镜下观察转移瘤病理切片。**结果** 38 只兔完成 CT 灌注扫描、DSA。CT 发现 6 只兔有 1 个肝转移瘤,32 只兔有多发肝转移瘤,大小为 1.2~2.1 cm,以环形强化为主要特征;DSA 显示 1 只兔有 1 个肝转移瘤,37 只兔有多发肝转移瘤,大小为 0.9~2.3 cm,以环形染色为主要特征。18 只兔(47.37%)经 DSA 发现的肝转移瘤数明显多于 CT,DSA 发现而 CT 未发现的肝转移瘤大小为 0.9~1.3 cm。DSA 和 CT 分别显示 37 只兔(97.37%)和 32 只兔(84.21%)有多发肝转移瘤($P < 0.01$)。CT 灌注扫描显示肝转移瘤边缘及中心区域 BV 值及 BF 值高于瘤周正常肝组织,转移瘤边缘高于中心区域($P < 0.01$);转移瘤边缘 HAP 值高于瘤周正常肝组织,PVP 值低于瘤周正常肝组织($P < 0.01$)。低倍镜下病理观察显示转移瘤中心为坏死组织和少量瘤细胞,坏死细胞排列松散,呈嗜碱性红染;外周为浓染的肿瘤细胞、结缔组织及炎性细胞,与正常组织边界欠清,可见丰富的新生毛细血管;10×40 倍镜下观察转移瘤中心坏死区为大量无核的坏死细胞,少量瘤细胞无胞质,仅可见浓染细胞核;外周为生长活跃的瘤细胞,形态不规则,胞核大而深染,胞质量少,可见丰富血窦。**结论** DSA 检出较小肝转移瘤优于 CT,肝转移瘤主要供血来源于肝动脉,肝转移瘤中心区域主要为坏死组织和少量瘤细胞,外周主要为生长活跃的瘤细胞和丰富的新生毛细血管,如此病理结构决定了肝转移瘤 CT 增强扫描以环形强化为主要特征,DSA 以环形染色为主要特征。

【关键词】 兔; VX2 肿瘤; 肝转移瘤模型; CT 灌注成像; 数字减影血管造影

中图分类号:R735.7 文献标志码:A 文章编号:1008-794X(2016)-07-0610-04

A comparative study of the imaging findings and pathological structures of VX2 liver metastases in experimental rabbits SHI Bo, LI Zhi-gang, LI Ya-zhou, WANG Yong-zhong, PING Yong, WU Yong-chao, HAO Xiao-guang. Department of Radiology, Forth Hospital of Hebei Medical University, Shijiazhuang, Hebei Province 050011, China

Corresponding author: LI Zhi-gang, E-mail: zhigangli9@yahoo.com.cn

【Abstract】 Objective To discuss the blood supply of the hepatic metastases in rabbit models and to analyze the relationship between the imaging findings and pathological structures. **Methods** Forty rabbits were used for this study. One ml of VX2 tumor strain cell suspension (concentration: $1 \times 10^7/\text{ml}$) was injected into the spleen. Fourteenth days after inoculation of tumor strain CT perfusion scan was performed, and fifteenth

days after inoculation DSA was carried out. The number and size of liver metastases were separately observed, the blood flow (BF) and blood volume (BV) of the tumor center, tumor periphery as well as normal liver tissue were measured on CT perfusion images, hepatic arterial fraction (HAF), hepatic arterial infusion volume (HAP) and portal vein perfusion volume (PVP) were calculated. The pathological sections were microscopically examined. **Results** CT perfusion scan and DSA were performed in 38 rabbits. On CT scan, only one hepatic metastatic lesion was detected in 6 rabbits, and multiple hepatic metastatic lesions were observed in 32 rabbits, the size of lesions was 1.2–2.1 cm, and ring enhancement was the main imaging characteristic. On DSA, only one hepatic metastatic lesion was seen in one rabbit, and multiple hepatic metastatic lesions were observed in 37 rabbits, the size of lesions was 0.9–1.3 cm, and the main feature was ring enhancement. In 18 rabbits (47.37%), the number of liver metastases demonstrated on DSA was obviously more than that showed on CT scan, The size of the lesions that were not displayed by CT scan was 0.9–1.3 cm. Multiple hepatic metastatic lesions were demonstrated by DSA and CT scan in 37 rabbits (97.37%) and 32 rabbits (84.21%) respectively. CT perfusion scan showed that BV and BF values measured at the lesion's periphery and center were higher than that measured at the normal liver tissue around the tumor, and BV and BF values at the lesion's center were higher than those at lesion's periphery ($P < 0.01$). HAP values of the lesion's periphery were higher than those of the normal liver tissue around the tumor, while PVP values of the lesion's periphery were lower than those of the normal liver tissue around the tumor ($P < 0.01$). Low magnification microscopic examination revealed that necrotic tissue and a small number of tumor cells were seen in the center of metastasis, the necrotic cells were loosely distributed and showed eosinophilic red dye; in the periphery of tumor dark stained cancer cells, connective tissue and inflammatory cells could be found, the lesion's boundary with normal tissue was less clear, and abundant new capillaries could be seen. Under microscope with 10×40 times magnification, a large number of necrotic cells and a small amount of tumor cells that showed dense nuclei and no cytoplasm were observed in the lesion's center; in the periphery of tumor there were irregularly-shaped and actively-growing cancer cells, which had big nucleus and less cytoplasm and were darkly stained; abundant blood sinuses were also seen. **Conclusion** DSA is superior to CT scan in detecting smaller hepatic metastasis; the main blood supply of hepatic metastases is from hepatic artery. In the central region of hepatic metastases there are mainly necrotic tissues and small amount of tumor cells, while at tumor's periphery there are mainly actively-growing cancer cells and abundant new capillaries; such pathological structures have determined that the ring-enhancement will undoubtedly be the main imaging feature of hepatic metastases on enhanced CT scan as well as on DSA. (J Intervent Radiol, 2016, 25: 610-613)

【Key words】 rabbit; VX2 tumor; liver metastatic tumor model; CT perfusion imaging; digital subtraction angiography

随着近年有效防治乙型肝炎,我国肝转移瘤在肝脏恶性肿瘤中的比例逐渐增加,肝转移瘤治疗越来越受重视^[1],影像学检查及介入栓塞治疗已成为肝转移瘤首选诊断与治疗方法^[2]。本实验通过构建兔肝转移瘤模型,探讨肝转移瘤血供来源及其影像学表现与病理结构的关系。

1 材料与方法

取新西兰大白兔 40 只,雌雄不限,体重 2.8~3.5 kg;于脾脏种植 VX2 肿瘤细胞悬液 1 ml,浓度为 $1 \times 10^7/\text{ml}$ ^[3]。接种瘤株后第 14 天作 CT 灌注扫描,

第 15 天作 DSA 造影^[4],随后处死动物,取肝转移瘤制成切片。

CT 灌注扫描设为 80 kV, 200 mA, 层厚 2.5 mm, 延时 5 s, 共扫描时间 12 s;灌注扫描间隔时间 1 s, 共扫描 5 次,采集 192 幅图像;对比剂碘佛醇注射速度为 1 ml/s,注射总量为 4 ml。将扫描所获图像及数据用 CT 软件包中肝肿瘤灌注模式作后处理,设定腹主动脉为流入动脉,门静脉为流入静脉,分别选取肝转移瘤边缘强化最明显部位、转移瘤中心区域及瘤周正常肝组织为兴趣区。CT 灌注扫描参数包括血流量(BF)、血容量(BV)、肝动脉供血分数(HAF)。

根据公式计算出肝动脉灌注量(HAP)和门静脉灌注量(PVP): $HAP=BF \times HAF$, $PVP=BF \times (1-HAF)$ 。

将麻醉后实验兔仰卧位固定于 DSA 机手术台上,显露并穿刺右侧股动脉,透视监视下将 2.2 F Stride 微导管分别选择至腹主动脉、腹腔干、脾动脉及肝固有动脉作造影,观察兔肝脏转移瘤血管造影表现。

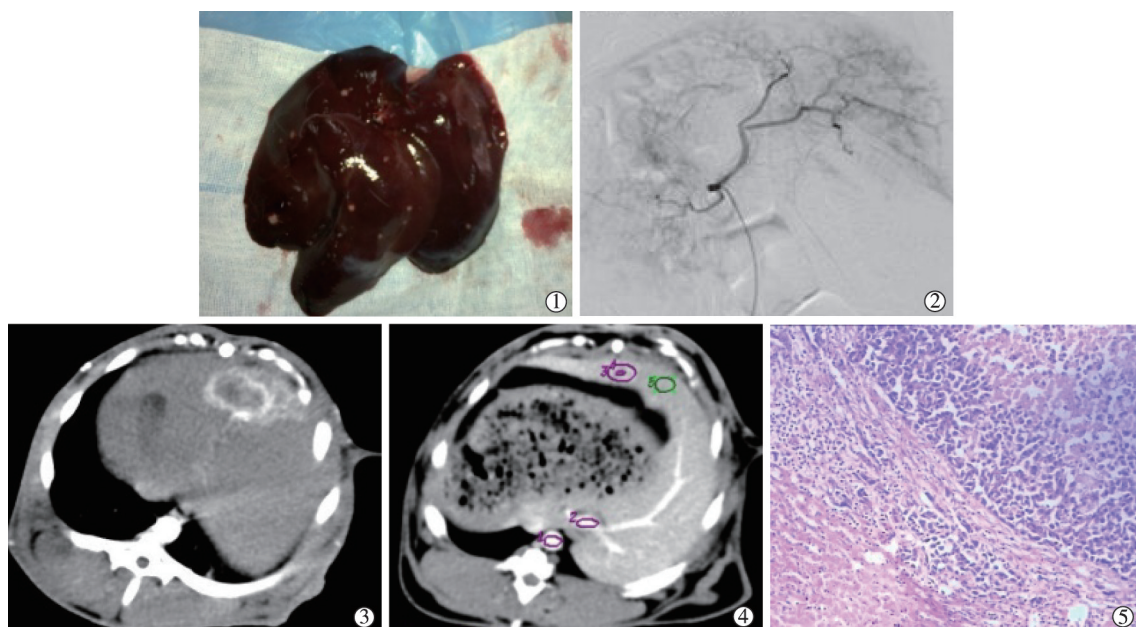
处死实验兔并取出肝脏组织,分离肝转移瘤,将转移瘤脱水、固定后制作苏木精-伊红(HE)染色切片,显微镜下观察转移瘤及周围组织结构。

2 结果

实验兔 40 只中 38 只完成 CT 灌注扫描、DSA 检查及病理切片检查,1 只于接种后 12 d 死亡,1 只

于 DSA 检查后死亡。CT 扫描显示 38 只实验兔中 6 只有 1 个肝转移瘤,30 只有 2~5 个脏转移瘤,2 只有 5 个以上肝转移瘤,大小为 1.2~2.1 cm,以环形强化为主要特征。DSA 显示 38 只实验兔中 1 只有 1 个肝转移瘤,25 只有 2~5 个肝转移瘤,12 只有 5 个以上肝转移瘤,大小为 0.9~2.3 cm,以环形染色为主要特征(图 1)。

18 只实验兔(47.37%)经 DSA 发现的肝转移瘤数明显多于 CT 扫描,DSA 发现而 CT 未发现的肝转移瘤大小为 0.9~1.3 cm。DSA 显示 37 只兔(97.37%)有多发肝转移瘤,CT 扫描显示 32 只兔(84.21%)有多发肝转移瘤例,两者间差异有统计学意义($P<0.01$)(表 1)。



①兔 VX2 肝转移瘤模型多发转移瘤;②兔肝固有动脉 DSA 造影示肝内多发转移瘤;③CT 扫描示兔肝内转移瘤呈环形强化;④CT 灌注扫描选取感兴趣区;⑤兔肝组织(10×10 倍)病理检查示肝转移瘤与瘤周正常肝组织边界欠清

图 1 兔 VX2 肝转移瘤模型影像与病理研究影像

表 1 38 只实验兔影像学发现肝转移瘤情况

影像	总数	1 个转移瘤	2~5 个转移瘤	>5 个转移瘤	多发转移瘤	多发转移瘤占比
CT 扫描/只	38	6	30	2	32	84.21%
DSA 造影/只	38	1	25	12	37	97.37%*

注: * 与 CT 扫描相比, $P<0.01$

CT 灌注扫描显示,肝转移瘤边缘及中心区域 BV 值及 BF 值高于瘤周正常肝组织,转移瘤边缘高于中心区域($P<0.01$);转移瘤边缘 HAP 值高于瘤周正常肝组织, PVP 值低于瘤周正常肝组织($P<0.01$)(表 2)。

表 2 38 只实验兔肝转移瘤 CT 灌注扫描结果

参数	转移瘤中心区域	转移瘤边缘	瘤周正常肝组织	P 值
BF 值/(ml/min)	205.60±42.24	364.54±109.13*	185.24±90.37	0.003
BV 值/(ml/100 g)	21.87±6.89	39.54±8.03*	12.03±2.98	0.001
HAF 值	0.60±0.19	0.76±0.25*	0.22±0.16	0.001
HAP 值	122.95±79.22	278.14±116.05*	40.01±58.58	0.001
PVP 值	82.65±82.29	86.40±62.02*	145.22±106.22	0.001

注: * 与瘤周正常肝组织相比, $P<0.01$

共制作肝转移瘤 HE 染色病理组织蜡块 60 个。10×10 倍显微镜下观察显示,转移瘤中心为坏死组

组织和少量瘤细胞,坏死细胞排列松散,呈嗜碱性红染;外周为浓染的肿瘤细胞、结缔组织及炎性细胞,与正常肝组织边界欠清,可见丰富的新生毛细血管(图1);10×40倍显微镜下观察显示,转移瘤中心坏死区为大量无核的坏死细胞,少量瘤细胞无胞质,仅可见浓染细胞核;外周为生长活跃的瘤细胞,形态不规则,胞核大而深染,胞质量少,可见丰富血窦。

3 讨论

本研究 40 只实验兔中有 2 只未能完成实验,1 只于接种瘤株后 12 d 死亡,经解剖发现腹腔内有大量腹水,腹膜有大量结节,肝内未发现转移灶,致死原因可能与接种肿瘤细胞悬液后未进行有效压迫,细胞悬液流出造成腹膜种植相关;另 1 只于 DSA 造影后死亡,考虑系麻醉药物过量缘故。完成实验的 38 只兔经 DSA 造影显示多发肝转移瘤者(37 只, 97.37%)明显高于 CT 扫描(32 只,84.21%)。有 18 只实验兔(47.37%)经 DSA 显示肝转移瘤数目明显多于 CT,且多为较小转移瘤,表明 DSA 对较小肝转移瘤的检出优于 CT。

CT 灌注扫描显示,肝转移瘤边缘及中心区域 BV 值、BF 值均高于瘤周正常肝组织,说明肝转移瘤供血较正常肝组织更丰富;肝转移瘤边缘 BV 值、BF 值高于中心区域,说明肝转移瘤外周供血较中心区域丰富,这与转移瘤 CT 增强扫描为环形强化及 DSA 造影为环形染色相符;肝转移瘤边缘 HAP 值高于瘤周正常肝组织,而 PVP 值低于瘤周正常肝组织,说明正常肝组织供血更多来源于门静脉,而肝转移瘤主要供血来源于肝动脉。

典型的肝转移瘤 CT 增强扫描显像为环形强化,DSA 造影为环形染色^[5],本实验结果也充分证明这一点。镜下 HE 染色切片观察发现肝转移瘤中心区域主要为坏死组织和少量瘤细胞,外周主要为生长活跃的瘤细胞和丰富的新生毛细血管,这说明肝转移瘤边缘生长活跃、供血丰富;中心区域坏死较多,这与肝转移瘤边缘 BV 值和 BF 值高于中心区域,转移瘤 CT 增强扫描为环形强化及 DSA 造影为环形染色相符。

[参考文献]

- [1] Tanaka K, Maeda N, Osuga K, et al. In vivo evaluation of irinotecan-loaded QuadraSphere microspheres for use in chemoembolization of VX2 liver tumors[J]. J Vasc Interv Radiol, 2014, 25: 1727-1735.
- [2] Tian M, Lu W, Zhang R, et al. Tumor uptake of hollow gold nanospheres after intravenous and intra-arterial injection: PET/CT study in a rabbit VX2 liver cancer model[J]. Mol Imaging Biol, 2013, 15: 614-624.
- [3] Dai F, Zhang X, Shen W, et al. Liposomal curcumin inhibits hypoxia-induced angiogenesis after transcatheter arterial embolization in VX2 rabbit liver tumors[J]. Onco Targets Ther, 2015, 8: 2601-2611.
- [4] Joo I, Kim JH, Lee JM, et al. Early quantification of the therapeutic efficacy of the vascular disrupting agent, CKD-516, using dynamic contrast-enhanced ultrasonography in rabbit VX2 liver tumors[J]. Ultrasonography, 2014, 33: 18-25.
- [5] 周大勇, 王建华, 钱 晟, 等. 肝动脉化疗栓塞术对富血供肝转移瘤的疗效分析[J]. 介入放射学杂志, 2007, 16: 165-167.

(收稿日期:2015-11-17)

(本文编辑:边 伟)